Letter

Strongly anisotropic spin dynamics in magnetic topological insulators

A. Alfonsov,[1,*] J. I. Facio,[1,*] K. Mehlawat,[1,2,*] A. G. Moghaddam,[1,3] R. Ray,[1] A. Zeugner,[4] M. Richter,[1,5] J. van den Brink,[1,2] A. Isaeva,[1,6] B. Büchner,[1,2] and V. Kataev[1]

[1]*Leibniz Institute for Solid State and Materials Research, IFW Dresden, D-01069 Dresden, Germany*
[2]*Würzburg-Dresden Cluster of Excellence ct.qmat, TU Dresden, D-01062 Dresden, Germany*
[3]*Department of Physics, Institute for Advanced Studies in Basic Sciences (IASBS), Zanjan 45137-66731, Iran*
[4]*Faculty of Chemistry and Food Chemistry, TU Dresden, D-01062 Dresden, Germany*
[5]*Dresden Center for Computational Materials Science (DCMS), TU Dresden, D-01062 Dresden, Germany*
[6]*Van der Waals–Zeeman Institute, Institute of Physics, University of Amsterdam, 1098 XH Amsterdam, The Netherlands*

(Received 5 August 2020; revised 18 December 2020; accepted 3 May 2021; published 19 May 2021)

The recent discovery of magnetic topological insulators has opened new avenues to explore exotic states of matter that can emerge from the interplay between topological electronic states and magnetic degrees of freedom, be it ordered or strongly fluctuating. Motivated by the effects that the dynamics of the magnetic moments can have on the topological surface states, we investigate the magnetic fluctuations across the $(MnBi_2Te_4)(Bi_2Te_3)_n$ family. Our paramagnetic electron spin resonance experiments reveal contrasting Mn spin dynamics in different compounds, which manifests in a strongly anisotropic Mn spin relaxation in $MnBi_2Te_4$ while being almost isotropic in $MnBi_4Te_7$. Our density-functional calculations explain these striking observations in terms of the sensitivity of the local electronic structure to the Mn spin orientation, and indicate that the anisotropy of the magnetic fluctuations can be controlled by the carrier density, which may directly affect the electronic topological surface states.

DOI: 10.1103/PhysRevB.103.L180403

I. INTRODUCTION

The experimental discovery of antiferromagnetic topological insulators (AFTIs) in the van der Waals $(MnBi_2Te_4)(Bi_2Te_3)_n$ family [1,2] has provided a fertile new basis for the investigation of exotic phenomena rooted in the interplay between topology of the electronic structure and spontaneous symmetry breaking, such as the quantum anomalous Hall effect, the topological magnetoelectric effect, and chiral Majorana fermions [3–7]. The two compounds studied the most so far, $MnBi_2Te_4$ and $MnBi_4Te_7$, order antiferromagnetically with the A-type spin structure at Néel temperatures $T_N \sim 24$ K and $T_N \sim 13$ K, respectively [8–14]. In this phase, both the time-reversal (Θ) and primitive-lattice translational ($T_{1/2}$) symmetries are broken but their combination $S = \Theta T_{1/2}$ is preserved [15]. For temperatures T below T_N, the topological protection of the surface states depends on whether or not the surface is S symmetric. At higher T, even if S can be broken locally and temporarily, the surface spectrum is expected to be gapless for any surface due to the restoration of Θ in a statistical sense [16,17], Θ being an average symmetry. As it results from averaging over magnetic fluctuations, the interplay between these and the topological electronic surface states naturally depends on space and time scales.

Experimentally, surface states with an origin in the band inversion have been widely observed [1,2,12–14,18–29] but the details around the Dirac point are the subject of controversy. In particular, among experiments that show a gapped surface spectrum for $T < T_N$, whether the gap persists above T_N represents an important open question. Our previous experimental results suggested that the dynamics of the bulk localized Mn magnetic moments play a key role in $MnBi_2Te_4$ [1] as electron spin resonance (ESR) measurements at $T > T_N$ show that the relaxation of the Mn moments due to the exchange coupling with the conduction electrons is strongly anisotropic. This suggests a strong anisotropy of Mn spin fluctuations which may give rise to an instantaneous (on the timescale of ESR) polarization field at the surface, preventing the gap to close even at $T \gg T_N$ as observed on the much faster timescale of the ARPES experiment. Indeed, further recent work proposes that the topological gap above T_N remains open due to short-range magnetic fields generated by chiral spin fluctuations [30].

Certainly, firm and final establishment of a correspondence between the characteristics of the magnetic fluctuations of both conduction electrons and paramagnetic Mn spins and the surface gap is a formidable task given the current, rather unsettled, experimental situation with regard to the surface band structure in different ARPES experiments triggering different, sometimes controversial, interpretations. In this context it is of paramount importance to unravel in detail the nature of the magnetic fluctuations across the $(MnBi_2Te_4)(Bi_2Te_3)_n$ family, the understanding of which is currently lacking. In this paper, we address this particularly crucial issue. First, we present ESR results which show that the anisotropy of the Mn spin relaxation rate in the paramagnetic state varies enormously

*These authors contributed equally to this work.

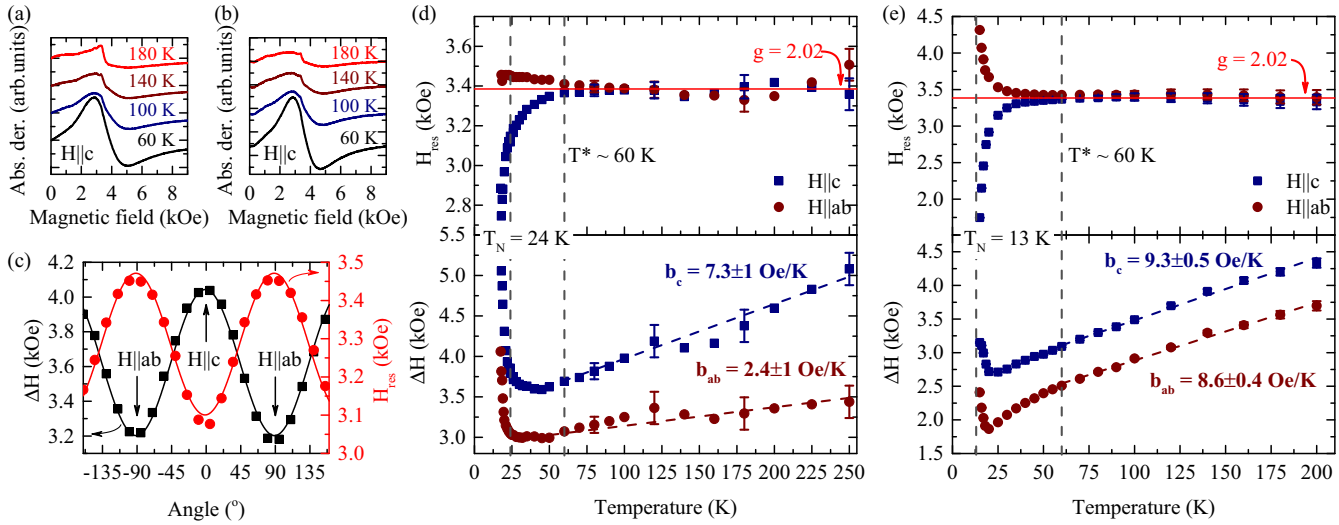

FIG. 1. ESR measurements. (a), (b) Temperature dependence of the spectra (field derivatives of the microwave absorption) with $H \parallel c$, for $MnBi_2Te_4$ and $MnBi_4Te_7$, respectively. (c) Angular dependence of the linewidth ΔH and of the resonance field H_{res} at $T = 20$ K for $MnBi_2Te_4$. Solid lines are fits of $\Delta H \sim [1 + \cos^2(\theta)]$ and $H_{res} \sim [1 + \sin^2(\theta)]$, where θ is the angle between H and the c axis. (d), (e) Temperature dependence of H_{res} and ΔH measured with two field orientations for $MnBi_2Te_4$ and $MnBi_4Te_7$, respectively. Dashed lines are fits of the Korringa dependence $\Delta H(T) = \Delta H_0 + bT$ while vertical dashed lines indicate the Néel temperature T_N and a crossover characteristic temperature T^* between two different types of temperature behavior of H_{res} and ΔH.

in the family being unprecedentedly large in $MnBi_2Te_4$ and nearly vanishing in $MnBi_4Te_7$. Second, based on density-functional calculations, we identify a critical role for the Mn spin dynamics played by the magnetic anisotropy of the electronic structure, which consistently explains the ESR data and further suggests that in doped semiconductors the carrier density can be used to tune the high-temperature anisotropy of the spin dynamics.

II. ESR EXPERIMENTAL RESULTS

Electron spin resonance (ESR) measurements on high-quality $MnBi_2Te_4$ and $MnBi_4Te_7$ single-crystalline samples synthesized and thoroughly characterized by x-ray diffraction and electron-dispersive x-ray spectroscopy in Refs. [13,31], respectively, were carried out at a microwave frequency of $\nu = 9.56$ GHz and at temperatures from 4 to 300 K using a commercial Bruker X-band spectrometer. The magnetic field H was swept from 0 to 9 kOe. The ESR signals have a well-defined asymmetric Dysonian shape [32,33], typical for conducting samples. This is indeed expected since Mn/Bi antisite intermixing is omnipresent in $MnBi_2Te_4$ ($Mn_{0.85}Bi_{2.1}Te_4$) and $MnBi_4Te_7$ ($Mn_{0.8}Bi_{4.1}Te_7$) crystals and acts as intrinsic self-doping [1,10,11,13,31,34]. Characteristic spectra are presented in Figs. 1(a) and 1(b). At high temperature, the line shape gets somewhat distorted due to an emerging small and narrow impurity peak which can be easily taken into account in the Dysonian fit. In order to precisely align the samples in the magnetic field parallel ($H \parallel c$) and normal ($H \parallel ab$) to the c axis, we have measured the angular dependence of the linewidth (ΔH) and of the resonance field (H_{res}) at a low temperature, which are exemplarily plotted in Fig. 1(c). They follow a typical $\Delta H \sim [1 + \cos^2(\theta)]$ (or $H_{res} \sim [1 + \sin^2(\theta)]$) dependence whose extrema correspond to the respective field geometries, as indicated in the figure.

The T dependence of H_{res} and of ΔH obtained from the Dysonian fits is shown for both field orientations on Fig. 1(d) for $MnBi_2Te_4$ and on Fig. 1(e) for $MnBi_4Te_7$. Due to a decrease of the intensity of the ESR signal with increasing temperature according to the Curie-Weiss law, the error bars of the fit increase correspondingly.

One can identify in Figs. 1(d) and 1(e) a crossover temperature $T^* \sim 60$ K which separates two different types of behavior of $H_{res}(T)$ and $\Delta H(T)$. At $T > T^*$, the resonance field is T independent and it has the same value (within error bars) for both directions of H. The resonance condition $h\nu = g\mu_B H_{res}$ yields the isotropic g factor $g = 2.02$ for both compounds. It is close to the spin-only value of $g_S \approx 2.0023$, as expected for the Mn^{2+} ($S = \frac{5}{2}$, $L = 0$) ion. In contrast, at $T < T^*$, H_{res} becomes significantly anisotropic. For $H \parallel ab$, the ESR line of $MnBi_2Te_4$ shifts slightly to higher fields, whereas for $H \parallel c$ it shifts strongly to smaller fields. Such behavior is typical for the antiferromagnetic (AFM) resonance modes [35]. However, these shifts commence well above $T_N \sim 24$ K and thus evidence the growth of the static, on the ESR timescale, short-range Mn-Mn spin correlations already in the paramagnetic regime, which is typical for the intrinsically low-dimensional van der Waals magnets (see, e.g., Refs. [36,37]). At $T < T_N$, the resonance line broadens and shifts further and finally disappears at $T \sim 17$ K since the AFM energy gap [35] becomes larger than the microwave excitation energy $h\nu$ at $\nu = 9.56$ GHz. $MnBi_4Te_7$ exhibits at $T < T^*$ a qualitatively similar behavior [Fig. 1(e)]. In this case, the shifts are strong for both field geometries, typical for a ferromagnet with an easy-axis anisotropy. Such ferromagnetic character of the low-T ESR response of $MnBi_4Te_7$ was established in our previous multifrequency ESR study [13].

The central observation in our ESR experiments is the contrasting behavior of the resonance line parameters in the high-temperature regime above $T^* \sim 60$ K. Here, an isotropic

and T-independent value of the resonance field evidences an uncorrelated, paramagnetic state of the Mn spin system in both compounds. The linewidth follows a linear temperature dependence $\Delta H(T) = \Delta H_0 + bT$ [Figs. 1(d) and 1(e)], characteristic of the Korringa relaxation of the localized magnetic moments by conduction electrons in the isothermal regime [38]. In this equation, ΔH_0 is the T-independent residual width due to, e.g., spin-spin interactions and magnetic field inhomogeneities, and the second term is the relaxation-driven T-dependent contribution [39]. Remarkably, for $MnBi_2Te_4$, the Korringa slope $b = d\Delta H(T)/dT$ [38,40] depends drastically on the direction of H. We obtain $b_c = 7.3 \pm 1$ Oe/K and $b_{ab} = 2.4 \pm 1$ Oe/K for $H \parallel c$ and $H \parallel ab$, respectively, yielding the ratio $b_{ab}/b_c = 0.33 \pm 0.14 \simeq 1/3$. In contrast, for $MnBi_4Te_7$, the values $b_c = 9.3 \pm 0.5$ Oe/K and $b_{ab} = 8.6 \pm 0.5$ Oe/K are very close, with the ratio $b_{ab}/b_c = 0.92 \pm 0.07$. While the overall larger b values in $MnBi_4Te_7$ are probably due to a higher doping level,[1] the very different anisotropy in the spin relaxation is more intriguing and will be discussed below.

III. ANISOTROPIC KORRINGA RELAXATION

In a magnetic resonance experiment, one measures the components of the dynamical magnetization $M_{x,y}$ of the paramagnetic species at their resonance frequency [41,42], transversal to the applied static magnetic field H. According to the so-called Bloch-Wangness-Redfield (BWR) theory, the width of the signal $\Delta H(T)$ is inversely proportional to the decay time τ of $M_{x,y}$ due to the relaxation processes caused by transversal and longitudinal fluctuating fields acting on the resonating spin ensemble [42–45]. In a metal, such fields are generated by conduction electrons exchange coupled to the localized spins (s-d coupling). This mechanism, known as the Korringa relaxation [38,40], gives rise to a linear in T increase of the linewidth and reads as, in the simplest case, $\Delta H(T) \sim 1/\tau(T) \sim [JD(\varepsilon_F)]^2 T$ [39]. Here, $D(\varepsilon_F)$ is the density of states (DOS) of itinerant electrons at the Fermi energy ε_F and J is the s-d coupling strength. In ordinary metallic systems, the Korringa slope $b = d\Delta H(T)/dT$ is found to be rather independent of the direction of H. There are only a few known examples of anisotropic Korringa relaxation in systems containing heavy elements with strong spin-orbit coupling (SOC) [46–48]. These include OsF_6-graphite intercalated compound, where the anisotropy was attributed to the anisotropy of J [46], and UPt_3, where an anisotropic relaxation rate in a nuclear magnetic resonance experiment [47] was explained by the anisotropic fluctuations of the heavy-fermion spins. Notably, in both cases one finds the ratio of the Korringa slopes $b_{ab}/b_c \gtrsim \frac{1}{2}$.[2] In this respect, the significantly smaller ratio $b_{ab}/b_c \simeq \frac{1}{3}$ found in $MnBi_2Te_4$ is unprecedented and remarkable.

To understand the sources of anisotropy in the Korringa relaxation, it is convenient to express the relaxation rate in terms of the frequency ω-dependent and wave-vector $\mathbf{q}$-dependent spin susceptibility $\chi_{i,i}(\omega, \mathbf{q})$ of conduction electrons, with $i = x, y, z$. Choosing the z axis along the direction of H, the relaxation rate reads as [49,50]

$$\frac{1}{\tau_z} = T \lim_{\omega\to 0} \frac{1}{\omega} \sum_{\mathbf{q}} \mathrm{Im}\left[2J_z^2\, \chi_{zz}(\omega, \mathbf{q}) + \sum_{i=x,y} J_i^2\, \chi_{ii}(\omega, \mathbf{q})\right], \tag{1}$$

where we have set $\hbar = k_B = 1$ and we have considered that the s-d exchange coupling consists of three different diagonal components J_i. An explicit calculation [see Supplemental Material (SM) [51]] yields

$$\frac{1}{\tau_z} = \pi T\left[2J_z^2\, |\mathcal{S}_z(\varepsilon_F)|^2 + \sum_{i=x,y} J_i^2\, |\mathcal{S}_i(\varepsilon_F)|^2\right], \tag{2}$$

$$|\mathcal{S}_i(\varepsilon)|^2 = \sum_{\nu\mathbf{k},\nu'\mathbf{k}'} \delta(\varepsilon - \varepsilon_{\nu\mathbf{k}})\delta(\varepsilon - \varepsilon_{\nu'\mathbf{k}'})\left|\mathcal{F}^{i,\nu\nu'}_{\mathbf{k}\mathbf{k}'}\right|^2, \tag{3}$$

where ν is a band index, $\mathbf{k}$ the momentum, and $|\mathcal{F}^{i,\nu\nu'}_{\mathbf{k}\mathbf{k}'}|^2$ denotes $\mathrm{Tr}[\mathcal{F}^{i,\nu\nu'}_{\mathbf{k}\mathbf{k}'}\mathcal{F}^{i,\nu'\nu}_{\mathbf{k}'\mathbf{k}}]$, with $\mathcal{F}^{i,\nu\nu'}_{\mathbf{k}\mathbf{k}'} = \langle u_{\nu\mathbf{k}}|\hat{\sigma}_i|u_{\nu'\mathbf{k}'}\rangle/2$ the matrix elements of the spin operator $\hat{\sigma}^i$ with respect to the spinor parts of Bloch functions $|u_{\nu\mathbf{k}}\rangle = a_{\nu\mathbf{k}}|\uparrow\rangle + b_{\nu\mathbf{k}}|\downarrow\rangle$. Without SOC, $\mathcal{F}^{i,\nu\nu'}_{\mathbf{k}\mathbf{k}'}$ is momenta independent and, therefore, $\mathcal{S}_i(\varepsilon) \equiv D(\varepsilon)$. If we further consider an isotropic J, the original Korringa result is recovered [40]. In general, SOC can give rise to anisotropy both in J_i and in $\mathcal{S}_i(\varepsilon_F)$, which in turn may lead to anisotropic relaxation rates, as indicated by Eq. (2).

Equation (2) was obtained in the zero magnetic field limit, which implies that the Larmor frequency of Mn spins ω_L is much smaller than the frequency of the spin fluctuations of the conduction electrons ω_{fl}. In this limit, Eq. (2) matches the BWR results expressing the fluctuating fields introduced in this theory as $\tau_0\overline{H_i^2} = TJ_i^2\, |\mathcal{S}_i(\varepsilon_F)|^2$ (see SM [51]), where the correlation time τ_0 in our problem is $1/\omega_{\mathrm{fl}}$. This connection provides a physical interpretation for the shape factors $\mathcal{S}_i$: They are the band-structure property that together with T and J_i determine the effective magnetic field exerted by the electron cloud on the Mn spins on a timescale τ_0. It further suggests an extension to the finite-field case $\omega_L \lesssim \omega_{\mathrm{fl}}$, which in the BWR theory yields a prefactor $\mathcal{A}_\omega \sim (1 + \omega_L^2/\omega_{\mathrm{fl}}^2)^{-1}$ for the second term in Eq. (2) [42].

Given the layered structure of these compounds, J_c and $\mathcal{S}_c$ can be significantly different from their in-plane counterparts J_{ab}, $\mathcal{S}_{ab}$.[3] In this case, the ratio of the relaxation times reads as

$$\frac{\tau_c}{\tau_{ab}} = \frac{1}{2}\frac{2 + \mathcal{A}_\omega(1+\zeta)}{\mathcal{A}_\omega + \zeta}, \tag{4}$$

where $\zeta = |J_c\mathcal{S}_c(\varepsilon_F)/J_{ab}\mathcal{S}_{ab}(\varepsilon_F)|^2$. If $\mathcal{S}_i(\varepsilon_F)$ is isotropic and $\omega_L/\omega_{\mathrm{fl}} \ll 1$, the remaining anisotropy due to that of J_i is bounded as $(\frac{1}{2})_{J_{ab}\to 0} < \tau_c/\tau_{ab} < (\frac{3}{2})_{J_c\to 0}$, posing a problem to account for the experimental result for $MnBi_2Te_4$, $b_{ab}/b_c = \tau_c/\tau_{ab} \simeq \frac{1}{3}$. Assuming a finite ratio $\omega_L/\omega_{\mathrm{fl}}$ which yields $\mathcal{A}_\omega <$

[1] This is supported by the difference in the room-temperature resistivity values ρ for these compounds: $MnBi_2Te_4$ has $\rho \sim 1.5$ mΩ cm [1] and $MnBi_4Te_7$ has $\rho \sim 0.31$ mΩ cm [13].

[2] Note that for the OsF_6-GIC this ratio $b_{ab}/b_c \gtrsim \frac{1}{2}$ is still true if the g-factor anisotropy, present in this compound, is not taken into account.

[3] We neglect anisotropy within the ab plane in all discussions and calculations.

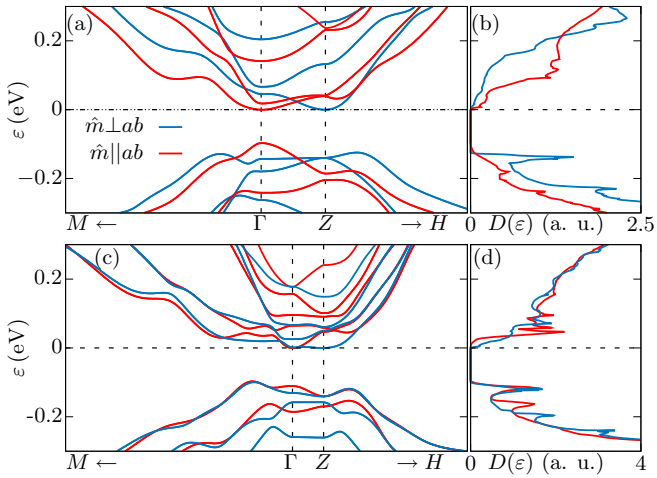

FIG. 2. (a), (b) Band structure and density of states, respectively, of $MnBi_2Te_4$ in the AFM phase for out-of-plane (blue) or in-plane (red) Mn magnetic moment direction. (c), (d) Analogous results for $MnBi_4Te_7$.

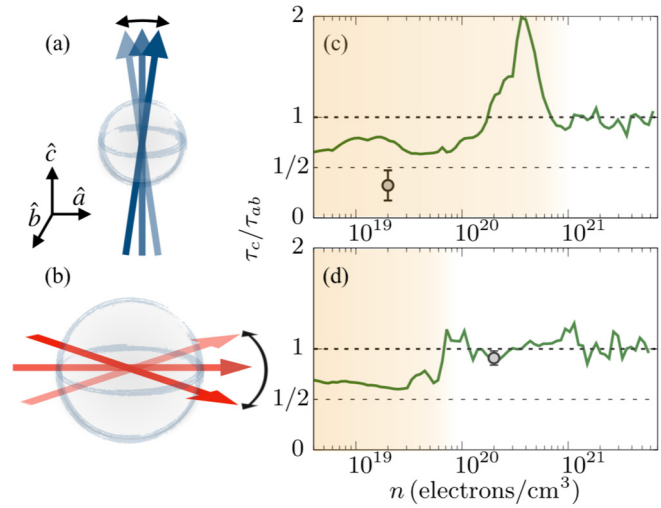

FIG. 3. (a), (b) Pictorial representation of the anisotropic spin dynamics. An out-of-plane Mn spin is accompanied by a relatively small carrier DOS (gray electron cloud) and, accordingly, has a relatively slow dynamics as compared to an in-plane Mn spin, accompanied by a larger DOS and presenting faster dynamics. (c), (d) Estimation of relaxation rate ratio as a function of the carrier density for $MnBi_2Te_4$ (c) and for $MnBi_4Te_7$ (d). The gray circles correspond to the experimental ESR data, estimating n from the Hall measurements on the same samples in Refs. [1,13], respectively.

1, the above limits can be surpassed, ultimately reaching $\tau_c/\tau_{ab} = \frac{1}{4}$ for $\omega_L = \omega_{fl}$ and $\zeta \gg 1$. However, that would require J to have an extreme Ising-type anisotropy with vanishing J_{ab} in $MnBi_2Te_4$ while being almost isotropic in $MnBi_4Te_7$.

Therefore, to understand the anisotropy of the Korringa relaxation in $MnBi_2Te_4$, it is necessary to analyze a possible anisotropy of the form factors $\mathcal{S}_i(\varepsilon_F)$ associated with the conduction electron cloud. This can be relevant when the carriers have a large SOC, as in the studied compounds. In such a case, for temperatures where the timescale of the dynamics of the Mn spins is longer than the timescale of conduction electrons, one may expect changes in the local electronic structure arising from the induced instantaneous polarization of the local moments, "frozen" on the fast electronic timescale, which can in turn affect the relaxation.

IV. BAND-STRUCTURE ANISOTROPY

We now explore this idea, assuming a large separation between timescales: The measured ESR occurs on the slowest scale ($\sim 10^{-10}$ s); on the intermediate scale ($\sim 10^{-13}...10^{-14}$ s), the Mn magnetic moment direction $\hat{m}$ fluctuates; on the fast scale ($\sim 10^{-15}$ s), the electronic system adapts to the local Mn spin direction and dissipates the excitation. Figures 2(a) and 2(b) present the energy bands and DOS of $MnBi_2Te_4$ in the AFM phase for different $\hat{m}$, and Figs. 2(c) and 2(d) show results for $MnBi_4Te_7$.[4] In order to prove that our approach is robust against the details of this model, we performed similar calculations for the FM state. In these calculations we find the same dependence of the DOS on the direction of the Mn magnetic moment as in the AFM model [51]. In both cases the sensitivity to $\hat{m}$ is significantly smaller in $MnBi_4Te_7$. For this compound, within planes perpendicular to $\Gamma - Z$, the bands are much less affected by $\hat{m}$, which naturally reflects in $D(\varepsilon)$. Such lesser sensitivity possibly originates in various "dilution" effects caused by the Mn-free quintuple layer in $MnBi_4Te_7$ [51].

In $MnBi_2Te_4$, for small electron doping, the DOS tends to be larger when $\hat{m} \parallel ab$. This tendency qualitatively matches the results of the ESR experiment, where, for $H \parallel c$, the in-plane part of the Mn dynamic magnetization $M_{x,y} = M_{a,b}$ is probed. For those Mn ions that have their spin essentially in plane, the local electronic structure near them is better described by the calculation with $\hat{m} \parallel ab$. The larger DOS in such case contributes to a faster relaxation rate of $M_{x,y}$ than in the configuration $H \parallel ab$, where $M_{x,y} = M_{a,c} = M_{b,c}$ is probed [Figs. 3(a) and 3(b)].

These ideas can be illustrated with the following ansatz for the shape factors [51]. We estimate them as $\mathcal{S}_i = \langle D^2_{ab} \rangle$ for $H \parallel c$ and as $\mathcal{S}_i = \langle D^2_{bc} \rangle$ for $H \parallel ab$, where $\langle D^2_{ij} \rangle$ is the squared effective DOS when $\hat{m}$ is along the direction i or j. Since the shape factors are defined by the electronic structure, it is worth stressing that the dependence on the direction of H does not come from the negligible H dependence of

[4]Density-functional (DFT) calculations were performed using the FPLO code [52], version 18.52 [53] in its fully relativistic mode. The generalized gradient approximation (GGA) was applied in the parameterization PBE96 [54]. We used GGA+U (atomic limit) with parameters $U = 2$ eV and $J = 1$ eV. We used a linear tetrahedron method with k meshes of $24 \times 24 \times 24$ (rhombohedral setup) and $22 \times 22 \times 4$ (hexagonal setup) subdivisions for $MnBi_2Te_4$ and $MnBi_4Te_7$, respectively. To compute the DOS, we used meshes of $60 \times 60 \times 60$ and $60 \times 60 \times 5$ subdivisions, respectively. Structural details are based on experimental lattice parameters (see Refs. [1,13]).

the band structure. Rather, the role of H, together with the radio-frequency field direction, is to *select* the particular kind of fluctuations. For different directions of H, the measured resonance originates in Mn ions with different $\hat{m}$. The associated shape factors, considering the locally distinct electronic structure, are accordingly different.

Neglecting a possible anisotropy of J and assuming the limit $\omega_L/\omega_{\rm fl} \ll 1$, so that the effects described are purely related to the band structure, this approach yields $\tau_c/\tau_{ab} = \langle D_{bc}^2\rangle/\langle D_{ab}^2\rangle$. Figures 3(c) and 3(d) show the estimated ratio τ_c/τ_{ab} as a function of the carrier density n for $MnBi_2Te_4$ and $MnBi_4Te_7$, respectively. Specifically, we consider $\langle D_{ab}^2\rangle = D_{\hat{m}\|ab}^2$ and $\langle D_{bc}^2\rangle = (D_{\hat{m}\|ab}^2 + D_{\hat{m}\|\hat{c}}^2)/2$, where the DOS are evaluated at fixed n. For comparison, our experimental ESR results are included as gray circles. The almost isotropic Korringa relaxation in $MnBi_4Te_7$ is well captured, whereas the anisotropy in $MnBi_2Te_4$ is underestimated. However, quantitative agreement may be achieved by considering an anisotropy of J or a finite Larmor frequency, as discussed above.

Interestingly, both compounds exhibit a crossover as a function of doping signaled by large deviations from $\tau_c/\tau_{ab} = 1$ at small n to nearly vanishing anisotropy at large n. It appears that the main difference between the compounds is the level of doping at which the crossover occurs. In particular, the samples of $MnBi_2Te_4$ and $MnBi_4Te_7$ lie on the anisotropic and isotropic sides of this crossover, respectively, in agreement with the ESR results. Reducing n in $MnBi_4Te_7$ by only one order of magnitude, potentially achievable by partial substitution of Bi by Sb [8], would recover the strong anisotropy $\tau_c < \tau_{ab}$, while a significant increase of n in $MnBi_2Te_4$ would change its type ($\tau_c > \tau_{ab}$) and eventually turn it to the isotropic limit ($\tau_c = \tau_{ab}$).

These results should be relevant for the interpretation of experiments in which the observed physical processes are not slow enough to average out the anisotropy of the Mn spin dynamics. This is, for instance, the case for the photoemission process in the nonadiabatic, sudden regime, which is typically associated with a timescale faster than 10^{-15} s. In particular, the much slower out-of-plane Mn spin dynamics in $MnBi_2Te_4$ indicates a larger out-of-plane dynamic polarization yielding a nonzero instantaneous magnetic field perpendicular to the sample surface, which could contribute to the persistence of an electronic gap in the paramagnetic phase. Our theoretical results suggest that appropriate engineering of the carrier density can favor the opposite or vanishing anisotropy and, hence, may provide a way to experimentally control the surface topological spectrum.

V. CONCLUSIONS

Our combined ESR and theoretical study shows that the Mn spin dynamics in magnetic topological insulators can be strongly anisotropic. The large spin-orbit coupling of conduction electrons plays a key role, making the local electronic structure strongly sensitive to Mn spin rotations, which in turn affects the Mn spin relaxation. Since the Mn spin dynamics can affect the topological surface states, our finding of the carrier density as a knob to control the anisotropy of magnetic fluctuations suggests a convenient way to tune the high-temperature surface spectrum of magnetic topological insulators. Altogether, our results open a perspective for exploring the magnetic dynamics and its interplay with nontrivial electronic structure in magnetic topological insulators and call for further investigations of the topological surface states at different timescales.

ACKNOWLEDGMENTS

This work was financially supported by the Deutsche Forschungsgemeinschaft (DFG) through Grant No. KA1694/12-1 and within the Collaborative Research Center SFB 1143 "Correlated Magnetism–From Frustration to Topology" (Project-id No. 247310070) and the Dresden-Würzburg Cluster of Excellence (EXC 2147) "ct.qmat-Complexity and Topology in Quantum Matter" (Project-id No. 39085490). J.I.F. acknowledges the support from the Alexander von Humboldt Foundation. K.M. acknowledges the Hallwachs-Röntgen Postdoc Program of ct.qmat for financial support. We thank U. Nitzsche for technical assistance.

[1] M. M. Otrokov, I. I. Klimovskikh, H. Bentmann, D. Estyunin, A. Zeugner, Z. S. Aliev, S. Gaß, A. U. B. Wolter, A. V. Koroleva, A. M. Shikin, M. Blanco-Rey, M. Hoffmann, I. P. Rusinov, A. Yu Vyazovskaya, S. V. Eremeev, Yu M. Koroteev, V. M. Kuznetsov, F. Freyse, J. Sánchez-Barriga, I. R. Amiraslanov *et al.*, Prediction and observation of an antiferromagnetic topological insulator, Nature (London) **576**, 416 (2019).

[2] Y. Gong, J. Guo, J. Li, K. Zhu, M. Liao, X. Liu, Q. Zhang, L. Gu, L. Tang, X. Feng *et al.*, Experimental realization of an intrinsic magnetic topological insulator, Chin. Phys. Lett. **36**, 076801 (2019).

[3] C.-Z. Chang, J. Zhang, X. Feng, J. Shen, Z. Zhang, M. Guo, K. Li, Y. Ou, P. Wei, Li-Li Wang, Z.-Q. Ji, Y. Feng, S. Ji, Xi Chen, J. Jia, Xi Dai, Z. Fang, S.-C. Zhang, K. He, Y. Wang *et al.*, Experimental observation of the quantum anomalous Hall effect in a magnetic topological insulator, Science **340**, 167 (2013).

[4] Q. L. He, L. Pan, A. L. Stern, E. C. Burks, X. Che, G. Yin, J. Wang, B. Lian, Q. Zhou, E. S. Choi, K. Murata, X. Kou, Z. Chen, T. Nie, Q. Shao, Y. Fan, S.-C. Zhang, K. Liu, J. Xia, and K. L. Wang, Chiral majorana fermion modes in a quantum anomalous hall insulator–superconductor structure, Science **357**, 294 (2017).

[5] Y. Tokura, K. Yasuda, and A. Tsukazaki, Magnetic topological insulators, Nat. Rev. Phys. **1**, 126 (2019).

[6] J. Jiang, D. Xiao, F. Wang, J.-H. Shin, D. Andreoli, J. Zhang, R. Xiao, Y.-F. Zhao, M. Kayyalha, L. Zhang *et al.*, Concurrence of quantum anomalous Hall and topological Hall effects in magnetic topological insulator sandwich heterostructures, Nat. Mater. **19**, 732 (2020).

[7] Y. Deng, Y. Yu, M. Z. Shi, Z. Guo, Z. Xu, J. Wang, X. H. Chen, and Y. Zhang, Quantum anomalous Hall effect in intrinsic magnetic topological insulator $MnBi_2Te_4$, Science **367**, 895 (2020).

[8] B. Chen, F. Fei, D. Zhang, B. Zhang, W. Liu, S. Zhang, P. Wang, B. Wei, Y. Zhang, Z. Zuo *et al.*, Intrinsic magnetic topological insulator phases in the Sb doped $MnBi_2Te_4$ bulks and thin flakes, Nat. Commun. **10**, 4469 (2019).

[9] D. Souchay, M. Nentwig, D. Günther, S. Keilholz, J. de Boor, A. Zeugner, A. Isaeva, M. Ruck, A. U. B. Wolter, B. Büchner *et al.*, Layered manganese bismuth tellurides with $GeBi_4Te_7$- and $GeBi_6Te_10$-type structures: towards multifunctional materials, J. Mater. Chem. C **7**, 9939 (2019).

[10] J.-Q. Yan, Q. Zhang, T. Heitmann, Z. Huang, K. Y. Chen, J.-G. Cheng, W. Wu, D. Vaknin, B. C. Sales, and R. J. McQueeney, Crystal growth and magnetic structure of $MnBi_2Te_4$, Phys. Rev. Mater. **3**, 064202 (2019).

[11] L. Ding, C. Hu, F. Ye, E. Feng, N. Ni, and H. Cao, Crystal and magnetic structures of magnetic topological insulators $MnBi_2Te_4$ and $MnBi_4Te_7$, Phys. Rev. B **101**, 020412(R) (2020).

[12] J. Wu, F. Liu, M. Sasase, K. Ienaga, Y. Obata, R. Yukawa, K. Horiba, H. Kumigashira, S. Okuma, T. Inoshita, and H. Hosono, Natural van der Waals heterostructural single crystals with both magnetic and topological properties, Sci. Adv. **5**, eaax9989 (2019).

[13] R. C. Vidal, A. Zeugner, J. I. Facio, Rajyavardhan Ray, M. H. Haghighi, A. U. B. Wolter, L. T. Corredor Bohorquez, F. Caglieris, S. Moser, T. Figgemeier, T. R. F. Peixoto, H. B. Vasili, M. Valvidares, S. Jung, C. Cacho, A. Alfonsov, K. Mehlawat, V. Kataev, C. Hess, M. Richter *et al.*, Topological Electronic Structure and Intrinsic Magnetization in $MnBi_4Te_7$: A Bi_2Te_3 Derivative with a Periodic Mn Sublattice, Phys. Rev. X **9**, 041065 (2019).

[14] C. Hu, K. N. Gordon, P. Liu, J. Liu, X. Zhou, P. Hao, D. Narayan, E. Emmanouilidou, H. Sun, Y. Liu *et al.*, A van der Waals antiferromagnetic topological insulator with weak interlayer magnetic coupling, Nat. Commun. **11**, 97 (2020).

[15] R. S. K. Mong, A. M. Essin, and J. E. Moore, Antiferromagnetic topological insulators, Phys. Rev. B **81**, 245209 (2010).

[16] I. C. Fulga, B. van Heck, J. M. Edge, and A. R. Akhmerov, Statistical topological insulators, Phys. Rev. B **89**, 155424 (2014).

[17] K. F. Garrity, S. Chowdhury, and F. M. Tavazza, Topological surface states of $MnBi_2Te_4$ at finite temperatures and at domain walls, Phys. Rev. Mater. **5**, 024207 (2021).

[18] R. C. Vidal, H. Bentmann, T. R. F. Peixoto, A. Zeugner, S. Moser, C.-H. Min, S. Schatz, K. Kißner, M. Ünzelmann, C. I. Fornari, H. B. Vasili, M. Valvidares, K. Sakamoto, D. Mondal, J. Fujii, I. Vobornik, S. Jung, C. Cacho, T. K. Kim, R. J. Koch *et al.*, Surface states and Rashba-type spin polarization in antiferromagnetic $MnBi_2Te_4$(0001), Phys. Rev. B **100**, 121104(R) (2019).

[19] Y.-J. Hao, P. Liu, Y. Feng, X.-M. Ma, E. F. Schwier, M. Arita, S. Kumar, C. Hu, R. Lu, M. Zeng, Y. Wang, Zhanyang Hao, H.-Y. Sun, K. Zhang, J. Mei, N. Ni, L. Wu, K. Shimada, C. Chen, Q. Liu *et al.*, Gapless Surface Dirac Cone in Antiferromagnetic Topological Insulator $MnBi_2Te_4$, Phys. Rev. X **9**, 041038 (2019).

[20] H. Li, S.-Y. Gao, S.-F. Duan, Y.-F. Xu, K.-J. Zhu, S.-J. Tian, J.-C. Gao, W.-H. Fan, Z.-C. Rao, J.-R. Huang, J.-J. Li, D.-Y. Yan, Z.-T. Liu, W.-L. Liu, Y.-B. Huang, Y.-L. Li, Y. Liu, G.-B. Zhang, P. Zhang, T. Kondo *et al.*, Dirac Surface States in Intrinsic Magnetic Topological Insulators $EuSn_2As_2$ and $MnBi_{2n}Te_{3n+1}$, Phys. Rev. X **9**, 041039 (2019).

[21] Y. J. Chen, L. X. Xu, J. H. Li, Y. W. Li, H. Y. Wang, C. F. Zhang, H. Li, Y. Wu, A. J. Liang, C. Chen, S. W. Jung, C. Cacho, Y. H. Mao, S. Liu, M. X. Wang, Y. F. Guo, Y. Xu, Z. K. Liu, L. X. Yang, and Y. L. Chen, Topological Electronic Structure and Its Temperature Evolution in Antiferromagnetic Topological Insulator $MnBi_2Te_4$, Phys. Rev. X **9**, 041040 (2019).

[22] P. Swatek, Y. Wu, L.-L. Wang, K. Lee, B. Schrunk, J. Yan, and A. Kaminski, Gapless Dirac surface states in the antiferromagnetic topological insulator $MnBi_2Te_4$, Phys. Rev. B **101**, 161109(R) (2020).

[23] Y. Hu, L. Xu, M. Shi, A. Luo, S. Peng, Z. Y. Wang, J. J. Ying, T. Wu, Z. K. Liu, C. F. Zhang, Y. L. Chen, G. Xu, X.-H. Chen, and J.-F. He, Universal gapless Dirac cone and tunable topological states in $(MnBi_2Te_4)_m(Bi_2Te_3)_n$ heterostructures, Phys. Rev. B **101**, 161113(R) (2020).

[24] K. N. Gordon, H. Sun, C. Hu, A. G. Linn, H. Li, Y. Liu, P. Liu, S. Mackey, Q. Liu, Ni Ni *et al.*, Strongly Gapped Topological Surface States on Protected Surfaces of Antiferromagnetic $MnBi_4Te_7$ and $MnBi_6Te_{10}$, arXiv:1910.13943.

[25] I. I. Klimovskikh, M. M. Otrokov, D. Estyunin, S. V. Eremeev, S. O. Filnov, A. Koroleva, E. Shevchenko, V. Voroshnin, A. G. Rybkin, I. P. Rusinov, M. Blanco-Rey, M. Hoffmann, Z. S. Aliev, M. B. Babanly, I. R. Amiraslanov, N. A. Abdullayev, V. N. Zverev, A. Kimura, O. E. Tereshchenko, K. A. Kokh *et al.*, Tunable 3d/2d magnetism in the $(MnBi_2Te_4)(Bi_2Te_3)_m$ topological insulators family, npj Quantum Mater. **5**, 54 (2020).

[26] L. Xu, Y. Mao, H. Wang, J. Li, Y. Chen, Yunyouyou Xia, Y. Li, D. Pei, J. Zhang, Huijun Zheng, K. Huang, Chaofan Zhang, S. Cui, A. Liang, W. Xia, H. Su, Sungwon Jung, C. Cacho, M. Wang, G. Li *et al.*, Persistent surface states with diminishing gap in $MnBi_2Te_4/Bi_2Te_3$ superlattice antiferromagnetic topological insulator, Sci. Bull. **65**, 2086 (2020).

[27] Xuefeng Wu, Jiayu Li, Xiao-Ming Ma, Yu Zhang, Y. Liu, C.-S. Zhou, J. Shao, Q. Wang, Y.-J. Hao, Y. Feng, E. F. Schwier, S. Kumar, H. Sun, P. Liu, K. Shimada, K. Miyamoto, T. Okuda, K. Wang, M. Xie, C. Chen *et al.*, Distinct Topological Surface States on the Two Terminations of $MnBi_4Te_7$, Phys. Rev. X **10**, 031013 (2020).

[28] R. C. Vidal, H. Bentmann, J. I. Facio, T. Heider, P. Kagerer, C. I. Fornari, T. R. F. Peixoto, T. Figgemeier, S. Jung, C. Cacho, B. Büchner, J. van den Brink, C. M. Schneider, L. Plucinski, E. F. Schwier, K. Shimada, M. Richter, A. Isaeva, and F. Reinert, Orbital Complexity in Intrinsic Magnetic Topological Insulators $MnBi_4Te_7$ and $MnBi_6Te_{10}$, Phys. Rev. Lett. **126**, 176403 (2021).

[29] Na Hyun Jo, L.-L. Wang, R.-J. Slager, J. Yan, Y. Wu, K. Lee, B. Schrunk, A. Vishwanath, and A. Kaminski, Intrinsic axion insulating behavior in antiferromagnetic $MnBi_6Te_{10}$, Phys. Rev. B **102**, 045130 (2020).

[30] A. M. Shikin, D. A. Estyunin, I. I. Klimovskikh, S. O. Filnov, E. F. Schwier, S. Kumar, K. Miyamoto, T. Okuda, A. Kimura, K. Kuroda, K. Yaji, S. Shin, Y. Takeda, Y. Saitoh, Z. S. Aliev, N. T. Mamedov, I. R. Amiraslanov, M. B. Babanly, M. M. Otrokov, S. V. Eremeev *et al.*, Nature of the Dirac gap modulation and surface magnetic interaction in axion antiferromagnetic topological insulator $MnBi_2Te_4$, Sci. Rep. **10**, 13226 (2020).

[31] A. Zeugner, F. Nietschke, A. U. B. Wolter, S. Gaß, R. C. Vidal, T. R. F. Peixoto, D. Pohl, C. Damm, A. Lubk, R. Hentrich, S. K. Moser, C. Fornari, C. H. Min, S. Schatz, K. Kißner, M. Ünzelmann, M. Kaiser, F. Scaravaggi, B. Rellinghaus, K.

Nielsch *et al.*, Chemical aspects of the candidate antiferromagnetic topological insulator $MnBi_2Te_4$, Chem. Mater. **31**, 2795 (2019).

[32] G. Feher and A. F. Kip, Electron Spin Resonance Absorption in Metals. I. Experimental, Phys. Rev. **98**, 337 (1955).

[33] F. J. Dyson, Electron spin resonance absorption in metals. II. theory of electron diffusion and the skin effect, Phys. Rev. **98**, 349 (1955).

[34] A. Tan, V. Labracherie, N. Kunchur, A. U. B. Wolter, J. Cornejo, J. Dufouleur, B. Büchner, A. Isaeva, and R. Giraud, Metamagnetism of Weakly Coupled Antiferromagnetic Topological Insulators, Phys. Rev. Lett. **124**, 197201 (2020).

[35] E. A. Turov, in *Physical Properties of Magnetically Ordered Crystals*, edited by A. Tybulewicz and S. Chomet (Academic, New York, 1965).

[36] J. Zeisner, A. Alfonsov, S. Selter, S. Aswartham, M. P. Ghimire, M. Richter, J. van den Brink, B. Büchner, and V. Kataev, Magnetic anisotropy and spin-polarized two-dimensional electron gas in the van der Waals ferromagnet $Cr_2Ge_2Te_6$, Phys. Rev. B **99**, 165109 (2019).

[37] J. Zeisner, K. Mehlawat, A. Alfonsov, M. Roslova, T. Doert, A. Isaeva, B. Büchner, and V. Kataev, Electron spin resonance and ferromagnetic resonance spectroscopy in the high-field phase of the van der Waals magnet $CrCl_3$, Phys. Rev. Mater. **4**, 064406 (2020).

[38] S. E. Barnes, Theory of electron spin resonance of magnetic ions in metals, Adv. Phys. **30**, 801 (1981).

[39] The linear in temperature Korringa relaxation is the unique fingerprint of the relaxation of the localized d states via the exchange coupling to the conduction electrons. Other relaxation channels are either T independent (e.g., dipole-dipole or exchange interactions) or strongly nonlinear in T (spin-phonon relaxation) [41]. The latter mechanism is inactive for Mn^{2+} due to the absence of the orbital moment.

[40] J. Korringa, Nuclear magnetic relaxation and resonnance line shift in metals, Physica (Amsterdam) **16**, 601 (1950).

[41] A. Abragam and B. Bleaney, *Electron Paramagnetic Resonance of Transition Ions* (Oxford University Press, Oxford, 2012).

[42] C. P. Slichter, *Principles of Magnetic Resonance*, Springer Series in Solid-State Sciences (Springer, Berlin, 1996).

[43] R. K. Wangsness and F. Bloch, The Dynamical Theory of Nuclear Induction, Phys. Rev. **89**, 728 (1953).

[44] F. Bloch, Dynamical Theory of Nuclear Induction. II, Phys. Rev. **102**, 104 (1956).

[45] A. G. Redfield, On the Theory of Relaxation Processes, IBM J. Res. Dev. **1**, 19 (1957).

[46] D. Vaknin, D. Davidov, V. Zevin, and H. Selig, Anisotropy and two-dimensional effects in the ESR properties of OsF_6-graphite intercalation compounds, Phys. Rev. B **35**, 6423 (1987).

[47] J. P. Vithayathil, D. E. MacLaughlin, E. Koster, D. Ll. Williams, and E. Bucher, Spin fluctuations and anisotropic nuclear relaxation in single-crystal UPt_3, Phys. Rev. B **44**, 4705 (1991).

[48] V. Kataev, U. Schaufuß, F. Murányi, A. Alfonsov, M. Doerr, M. Rotter, and B. Büchner, Magnetic anisotropy of the spin-antiferromagnet $GdNi_2B_2C$ probed by high-frequency ESR, J. Phys.: Conf. Ser. **150**, 042086 (2009).

[49] T. Moriya, The effect of electron-electron interaction on the nuclear spin relaxation in metals, J. Phys. Soc. Jpn. **18**, 516 (1963).

[50] R. E. Walstedt and A. Narath, Relaxation of local-moment nuclei in metals, Phys. Rev. B **6**, 4118 (1972).

[51] See Supplemental Material at http://link.aps.org/supplemental/10.1103/PhysRevB.103.L180403 for (i) derivation of Eq. (2), (ii) a discussion on the shape factors, and (iii) further details on the DFT results.

[52] K. Koepernik and H. Eschrig, Phys. Rev. B **59**, 1743 (1999).

[53] https://www.fplo.de/.

[54] J. P. Perdew, K. Burke, and M. Ernzerhof, Phys. Rev. Lett. **77**, 3865 (1996).